Fusion Engineering and Design 146 (2019) 765–769

Contents lists available at ScienceDirect

Fusion Engineering and Design

journal homepage: www.elsevier.com/locate/fusengdes

Modelling of MAST upgrade neutral beam re-ionization and the impact on the beamline ducts and in-vessel components

Alastair John Shepherd*, R. Akers, A. Barth, I.E. Day, G. Fishpool, R. McAdams, R. Tivey, R. Verhoeven

CCFE, Culham Science Centre, Abingdon, Oxon, OX14 3DB, UK

ARTICLE INFO

Keywords:
MAST-U
Neutral beam injection
Re-ionization
Duct liners

ABSTRACT

We describe modelling of neutral beam re-ionization along the MAST-U beamlines and into the MAST-U vessel, within a field envelope applicable to the operational space of the machine. Monte-Carlo simulations using the MAGNET code give the re-ionized power loading on both beamline ducts, which was used to position thermocouples on the duct liners. Thermal and structural analysis of the duct liners has been carried out using ANSYS.

The potential for significant amounts of re-ionized power entering the MAST-U vessel has resulted in the installation of graphite tile plating at the end of the ducts, compatible with co-injection. The power loading on these plates and other in-vessel components as modelled by MAGNET has been compared to the LOCUST code. Analysis has confirmed that the graphite tiles are compatible with core scope operation.

1. Introduction

Neutral beam injection (NBI) is one of the primary auxiliary heating systems for tokamak plasmas. Once the neutral beam leaves the neutraliser collisions with background neutral particles in the beamline and tokamak vessel re-ionizes part of the neutral beam. These particles can be deflected by the tokamak magnetic field, potentially damaging unshielded components.

The Mega Amp Spherical Tokamak Upgrade (MAST-U) has two Positive Ion Neutral Injectors (PINIs), one injecting power to be deposited close to the magnetic axis of the plasma (on-axis, South) and one injecting power that is deposited further out in the plasma (off-axis, Southwest). Each injector has been designed to run for up to 5 s [1], with 2 s of neutral beam required for the initial MAST-U experimental campaign. The increase in neutral beam pulse length and the increase in complexity of the in-vessel hardware compared to MAST increases the risk posed by re-ionization to the beamline ducts and in-vessel components.

2. Beamline re-ionization

A schematic of the MAST-U South beamline (with the Southwest beamline functionally identical) is given in Fig. 1. The MAST-U PINIs can extract a deuterium beam of 65 A at 75 kV [2], which is then re-ionized by neutral particles in the beamline, with the re-ionized power P_R given by

$$P_R = \sum_i P_{Ni}(1 - e^{(-\Pi\sigma)}) \quad (1)$$

Where P_{Ni} is the neutral beam power for a given energy species (full, half, third), Π is the target density and σ the re-ionization cross section.

An example beamline gas profile along the getter pumped MAST beamlines for an input flow of 30 mbarl/s (source and neutraliser gas) and a MAST vessel density of $2 \times 10^{18}\,m^{-3}$ has been calculated previously using the Monte-Carlo N-Particle transport code MCNP [3]. Similar gas profiles are expected in the MAST-U beamlines, with the new design of bend magnet and residual ion dumps not expected to have a significant impact on pumping. Considering the full, half and third energy neutral fractions (84.5%, 10.8%, 4.7% for a supercusp PINI at 75 kV/65 A), the target density calculated from the MAST beamline gas profile and the relevant cross sections [4] gives 239 kW of re-ionised power from the bend magnet to a point 0.4 m beyond the downstream duct liner. This re-ionized power, deflected by the MAST-U field, has the potential to impact on the duct liners and in-vessel components.

3. Representative MAST-U field

For the purposes of this study only MAST-U core scope was

* Corresponding author.
E-mail address: Alastair.Shepherd@ukaea.uk (A.J. Shepherd).

https://doi.org/10.1016/j.fusengdes.2019.01.076
Received 2 October 2018; Received in revised form 21 December 2018; Accepted 12 January 2019
Available online 23 January 2019

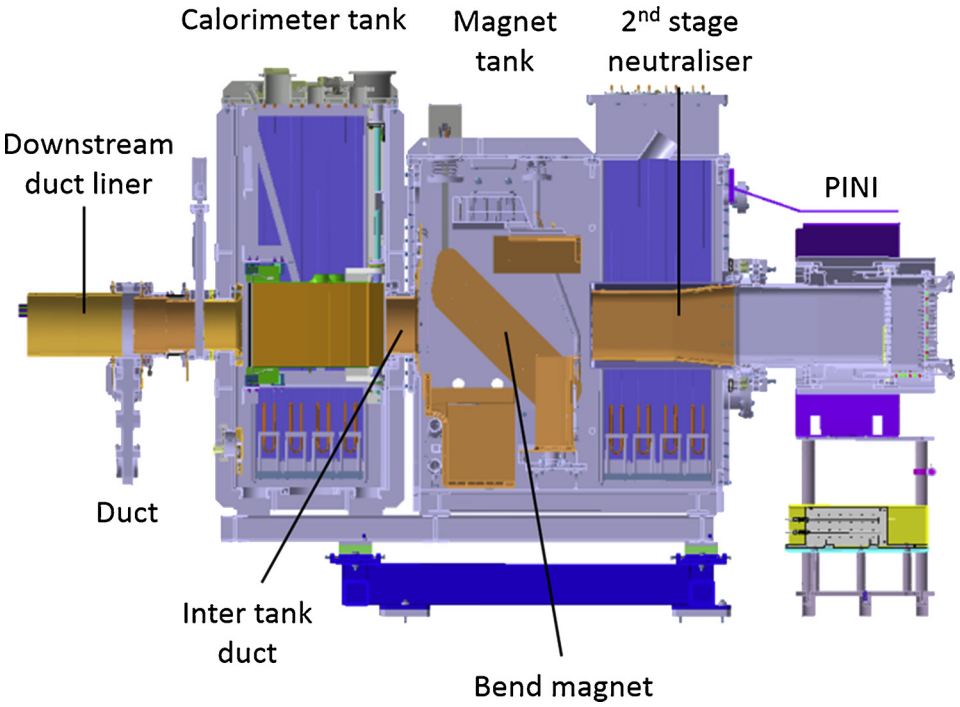

Fig. 1. Schematic of the MAST-U South beamline.

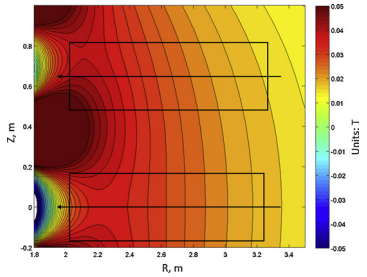

Fig. 2. Vertical component of the poloidal field for the chosen MAST-U equilibrium, I_p 2 MA. South (z = 0 m) and Southwest (z = 0.65 m) ducts and beam direction indicated.

considered, with the plasma current anticlockwise and NBI co-injected, as this covers the initial period of MAST-U operation. A representative 2 MA plasma was chosen that provided an upper limit for the poloidal field in the beamline ducts. The vertical component of the poloidal field is shown in Fig. 2. Being the main component perpendicular to the two beams and positive beyond the poloidal field coils the poloidal field bends ions in the beamlines to the right. The toroidal field, running clockwise, provides a horizontal field directed to the left in the ducts bending ions upwards.

The poloidal and toroidal fields were scaled with plasma current I_P and rod current (total current running through the 24 toroidal field conductors) I_R respectively, to study the bounding cases. For core scope I_P was scaled from 0.4 MA to 1 MA (upper limit 2 MA) and I_R from 1.44 MA to 2.4 MA (upper limit 3.192 MA). The lower limit for I_R was chosen to prevent re-ionized particles leaving the duct from hitting the poloidal field coils, while still allowing the toroidal field to be scaled by a factor of 1.7 in core scope.

4. NBI ducts

4.1. Re-ionized power loading

The re-ionized power loading on the beamline ducts and in-vessel components has been modelled using the MAGNET Monte-Carlo code. MAGNET calculates the re-ionized power produced along the beamline using Eq. (1), using a starting neutral beam profile that considers the focusing of the beam from the ground grid and the beamlet divergence. The deflection of the re-ionized particles in the MAST-U field is tracked until the particles collide with a surface. In MAGNET the circular copper duct liners are modelled as eight planes parallel to the inner surface, forming a series of octagonal tubes.

The highest modelled re-ionized power loading on the South and Southwest downstream duct liners occurs for a field with rod current of 2.4 MA and plasma current of 0.4 MA, with the re-ionized power footprint on the downstream liner shown in Fig. 3. The lower poloidal field component allows the highest proportion of re-ionized power to reach the end of the duct, where the high toroidal field bends the power upwards onto the lip of the top right surface. For the South beamline 92.3 kW of re-ionized power lands on the three duct liners, with a peak power density of 3.1 MW/m^2 on the downstream liner. For the Southwest beamline the duct loading is 106.7 kW with a peak power density of 3.5 MW/m^2.

Increasing the poloidal field component by scaling the plasma current to 1.0 MA spreads the power upstream along the right of the duct liners. For the South and Southwest ducts, the re-ionized power loading is 128.2 kW and 139.2 kW respectively, with a peak power density on the downstream liner of 1.4 MW/m^2 and 1.5 MW/m^2.

4.2. Thermal and structural analysis

A transient thermal model in ANSYS [5] has been used to assess the thermal impact of re-ionized power loading on the duct liner. The re-ionized power loading maps given in Fig. 3 were projected onto a model of the downstream liner, assumed to be pure copper, with inter-pulse cooling represented by convection on the outside of the liner. For each re-ionized power map three loading cases have been considered; a 0.5 s, 2 s and 5 s pulse, with multiple cycles applied to assess thermal ratcheting. For the 0.5 s and 2 s pulses a 15-minute cooling period between pulses was applied and 30 min between 5 s pulses, as this is the expected minimum pulse frequency with NBI. In each case the temperature was found to stabilize, with the results of the Southwest duct liner,

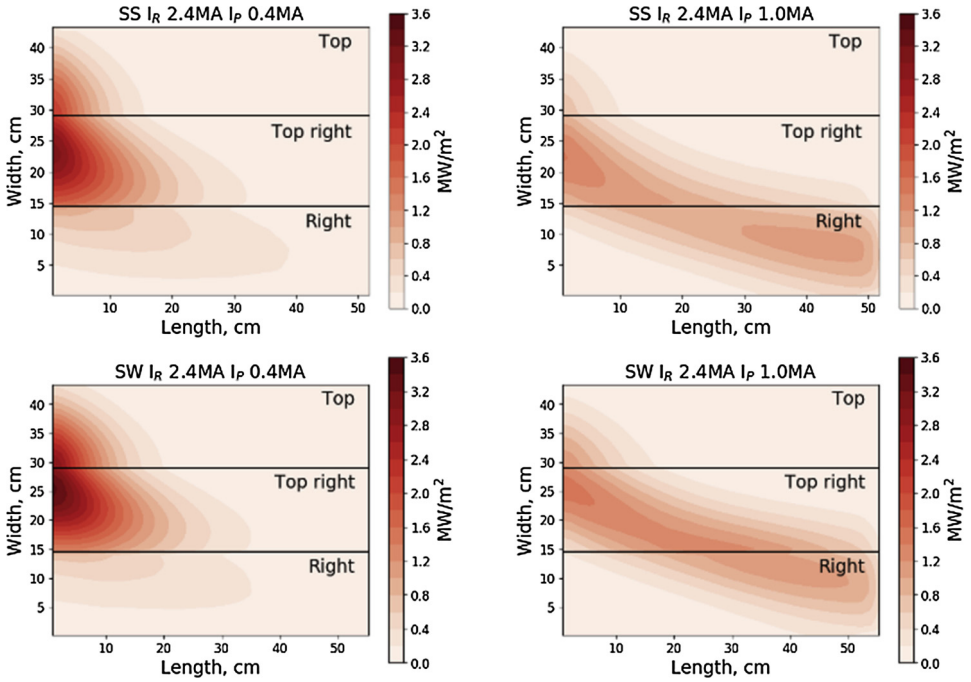

Fig. 3. Re-ionized power loading on the South (SS) and Southwest (SW) top, top right and right downstream duct liner MAGNET surfaces. Left in each plot is the end of the duct.

Table 1
Southwest downstream Cu duct liner thermal and structural analysis results.

I_R (MA)	I_P (MA)	Pulse length (s)	Max temp (°C)	vMises stress (MPa)	Yield strength (MPa)	Peak plastic strain (%)
2.4	0.4	0.5	97.2	43.9	49.9	0.04
		2.0	197.4	43.6	46.5	0.08
		5.0	323.7	42.1	36.0	0.24
	1.0	0.5	55.0	39.3	45.2	0.003
		2.0	100.6	43.5	49.7	0.06
		5.0	197.7	43.2	47.9	0.15

which has the highest peak power density, given in Table 1.

The thermal results have been applied to an ANSYS static structural model to assess the behavior of the duct liner under the re-ionized heat load. The von-Mises stress and peak plastic strain for the Southwest cases are given in Table 1 with example analysis shown in Fig. 4. The flange is not shown in the stress analysis as boundary conditions caused local high stresses. For pulses up to 2 s no yielding of the duct liner is observed, with the von-Mises stress below the yield strength for a pure copper tube at the given temperature, taken from SDC-IC A.S30.2.2 [6]. Some yielding occurs for 5 s pulses where the strain exceeds 0.2%.

5. In-vessel protection

For the low poloidal field cases shown in Fig. 3 some of the re-ionized power born in the beamlines misses the duct liner and enters the vessel. With a low toroidal field this proportion increases further, and with a high neutral pressure in the vessel (2×10^{18} m^{-3}) this can pose serious problems for in-vessel components. As mentioned in section 3 having a minimum rod current of 1.44 MA pulls the worst of the re-ionized power away from the poloidal field coils but this can still leave significant amounts of power entering the vessel.

5.1. Re-ionized power loading

To catch the re-ionized power leaving the duct graphite tiles have been placed at the end of the duct in the top right quadrant, extending to the poloidal field coils. Fig. 5 shows the South protection tiles, with the Southwest tiles similar in design. Each tile is mounted to a bracket by one fixing bolt, allowing the tiles to bend and relieving stress from the mounting. A steel plate has been placed under the upper P5 coil to provide protection from re-ionized particles born in vessel. For the South protection tiles limiters have been added to protect the tiles from halo currents. The Edge Localized Mode (ELM) coils provide similar protection for the Southwest protection tiles.

Fig. 6 shows the re-ionized power on the South graphite tiles numbered in Fig. 5, for two field cases with a plasma current of 0.4 MA. For a rod current of 1.44 MA 115.1 kW of re-ionized power lands on the tiles, with a peak power density of 3.4 MW/m^2 on tile 4. Increasing I_R to 2.4 MA pulls the power closer to the duct exit, reducing the total power on the tiles to 92.3 kW while increasing the peak power density to 4.2 MW/m^2 on tile 2.

5.2. Thermal and structural analysis

The thermal and structural behavior of a single 2158 P T graphite tile due to re-ionized loading has been investigated using ANSYS. Four potentially limiting cases have been analyzed; profile with a peak of 8 MW/m^2 for 2 s, 8 MW/m^2 for 5 s, 8 MW/m^2 for 2 s centered on the fixing hole, uniform 4 MW/m^2 over half the tile for 2 s.

Each load was applied over many cycles, with 30 min of radiative cooling between each cycle, reaching a steady base temperature. The peak transient temperature, tensile and compressive stress are given in Table 2 with an example of the analysis shown in Fig. 7. All the cases except 8 MW/m^2 for 5 s fall within the applied limits of 1300 °C, 15 MPa (tensile) and 30 MPa (compressive), which are below values known to cause failure in graphite tiles. For the loads given in Section 5.1 the tiles should remain below the limits for 5 s pulses.

6. MAGNET comparison to LOCUST

To benchmark the MAGNET results the MAST-U beamline re-ionization has been modelled using the LOCUST fast ion code [7]. Starting with neutral particles with position and velocity calculated from the

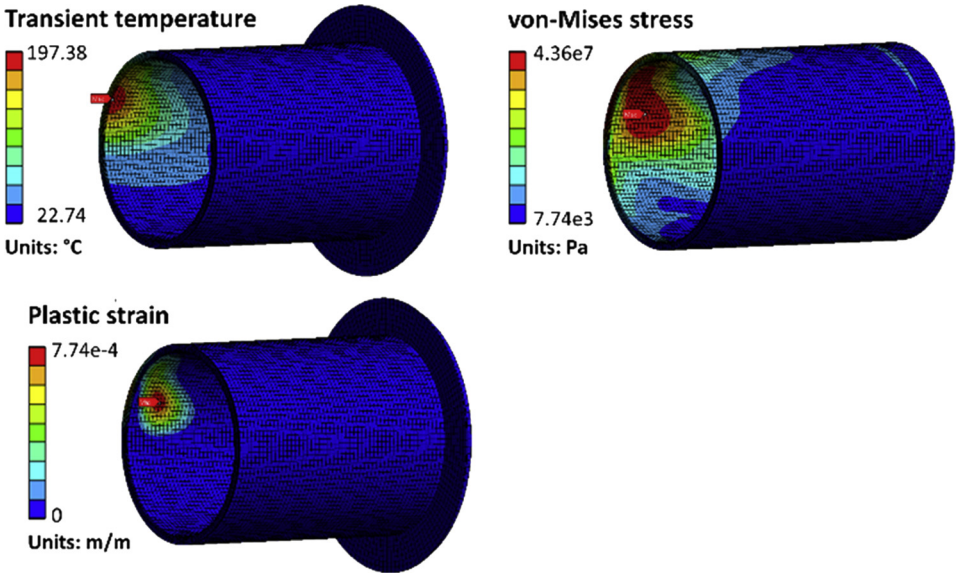

Fig. 4. Thermal and structural analysis of Southwest downstream duct liner for the I_R 2.4 MA I_P 0.4 MA field case with a 2 s beam pulse length.

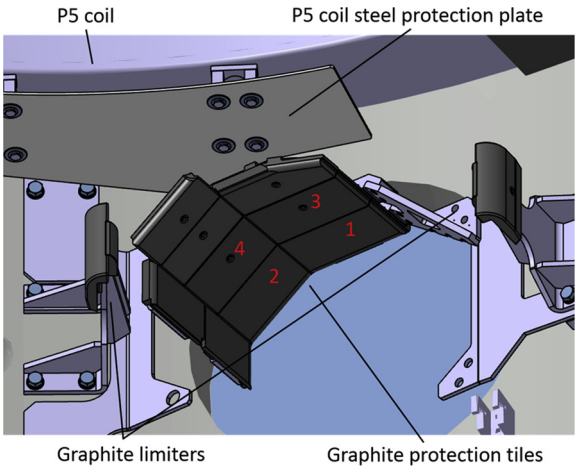

Fig. 5. Graphite protection tiles at the end of the South duct.

Table 2
Graphite tile thermal and stress analysis results.

Load (MW/m^2)	Pulse length (s)	Max temp (°C)	Base temp (°C)	Tensile stress (MPa)	Compressive stress (MPa)
8 (profile)	2	922	145	14.9	24.1
8 (profile)	5	1444	190	14.1	24.2
8 (shifted profile)	2	905	120	13.6	30.0
4 (uniform)	2	535	70	8.0	14.2

beamlet focusing, divergence and energy (full, half and third) re-ionized particles are created along the beamlines. The same pressure profile, re-ionization cross sections and poloidal field as MAGNET were used. The toroidal field was calculated separately for LOCUST, but representing the same field as used by MAGNET. Fig. 8 shows the re-ionized loading on the South graphite protection tiles calculated by the two codes for the same field case. The starting point in the simulations

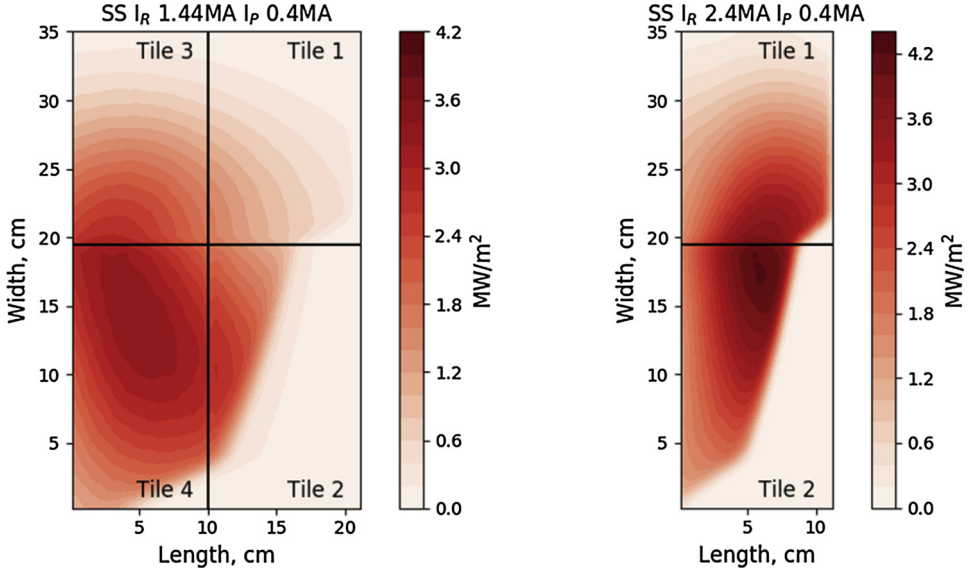

Fig. 6. Re-ionized power loading on the South graphite protection tiles.

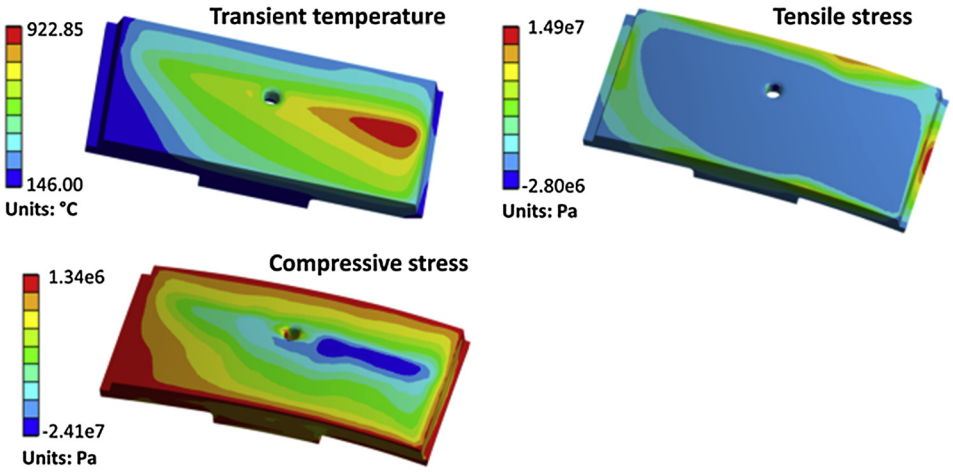

Fig. 7. Thermal and stress analysis of graphite tile under re-ionized load with a peak power density of 8 MW/m^2 for 2 s.

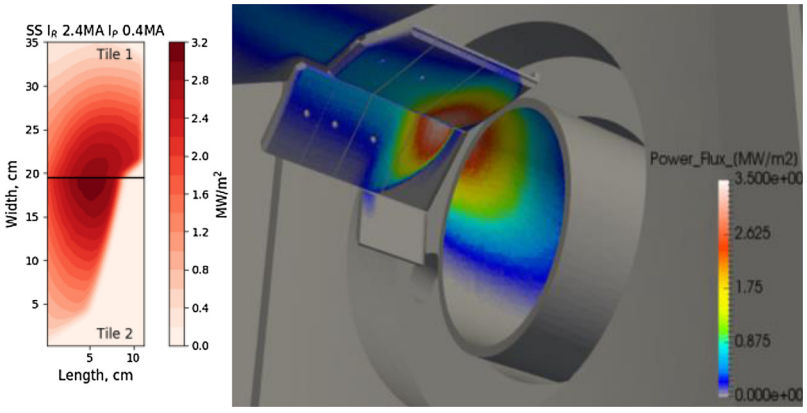

Fig. 8. Comparison between MAGNET and LOCUST. MAST-U field with I_R 2.4 MA, I_P 0.4 MA.

was the end of the inter tank duct, as the bend magnet field was not included in the LOCUST model. The two codes show broad agreement, with the position and profile of the re-ionized loading comparing well. LOCUST predicts a slightly higher peak power density of 3.5 MW/m^2 compared to 3.15 MW/m^2 for MAGNET.

7. Conclusions

Re-ionization of the neutral beam in the MAST-U beamlines has the potential to put significant amounts of power on the beamline duct and in-vessel components, depending on the MAST-U field. Modelling of the re-ionized power loading on the duct liners due to a representative field has given peak power densities of up to 3.5 MW/m^2. For some field cases significant amounts of re-ionized power misses the duct and enters the vessel. Graphite protection tiles have been installed to intercept this power, up to 4.2 MW/m^2, when the beams are operating in co-injection. Thermal and structural analysis has shown that the re-ionization loading on the ducts and graphite tiles is acceptable for 2 s pulses, making them compatible with the initial experimental campaign.

The re-ionization loading modelled by MAGNET has advised the positioning of thermocouples on the downstream duct liner. These will be monitored during commissioning and the first experimental campaign, along with thermocouples in the graphite protection tiles. LOCUST has been used to benchmark MAGNET, with broad agreement between the two. LOCUST, which can model MAST-U components in greater detail and quickly scan over field scenarios, is a promising tool for future re-ionization studies.

Additional modelling and analysis will need to be carried out to assess the protection needs for pulses longer than 2 s and scenarios outside of the initial MAST-U campaign. With the pumped divertor due to be delivered during the MAST-U Enhancements project lower torus neutral gas densities are expected, which will reduce the re-ionization in the ducts and in-vessel.

Acknowledgments

This work was funded by the RCUK Energy Programme [Grant number EP/P012450/1]. To obtain further information on the data and models underlying this paper please contact PublicationsManager@ukaea.uk.

References

[1] S.J. Gee, R. Baldwin, A. Borthwick, D. Ciric, G. Crawford, L. Hackett, et al., Fusion Eng. Des. 74 (2005) 403–407.
[2] D.A. Homfray, D. Ciric, V. Dunkley, R. King, D. Payne, M. Simmonds, et al., Overview of MAST neutral beam system performance, 23rd IEEE/NPSS Symposium on Fusion Engineering SOFE, (2009).
[3] R. McAdams, Control and calculation of the titanium sublimation pumping speed and re-ionisation in the MAST neutral beam injectors, Fusion Eng. Des. 90 (2015) 47–54.
[4] ORNL Redbooks, Atomic data for fusion, in: C.F. Barnett (Ed.), Collisions of H, H2, He and Li Atoms and Molecules with Atoms and Molecules, vol. 1, 1990 ORNL-6086.
[5] ANSYS Mechanical 18.2.
[6] ITER Structural Design Criteria for In-Vessel Components (SDC-IC), ITER Doc. G 74 MA 8 01-05-28 W0.2.
[7] R. Akers, et al., GPGPU Monte carlo calculation of gyro-phase resolved fast ion and n-state resolved neutral deuterium distributions, 39th EPS Conference & 16th Int. Congress on Plasma Physics, (2012) P5.088.